

Contents lists available at ScienceDirect

BioSystems

journal homepage: www.elsevier.com/locate/biosystems





Quantitative description of neuronal calcium dynamics in *C. elegans'* thermoreception

Zachary Mobille a,b, Rosangela Follmann c, Andrés Vidal-Gadea d, Epaminondas Rosa Jr. a,d,*

- ^a Department of Physics, Illinois State University, Normal, 61790, IL, USA
- ^b Department of Mathematics, Illinois State University, Normal, 61790, IL, USA
- ^c School of Information Technology, Illinois State University, Normal, 61790, IL, USA
- ^d School of Biological Sciences, Illinois State University, Normal, 61790, IL, USA

ARTICLE INFO

Keywords: Thermoreception Mathematical modeling Calcium C. elegans

ABSTRACT

The dynamical mechanisms underlying thermoreception in the nematode *C. elegans* are studied with a mathematical model for the amphid finger-like ciliated (AFD) neurons. The equations, equipped with Arrhenius temperature factors, account for the worm's thermotaxis when seeking environments at its cultivation temperature, and for the AFD's calcium dynamics when exposed to both linearly ramping and oscillatory temperature stimuli. Calculations of the peak time for calcium responses during simulations of pulse-like temperature inputs are consistent with known behavioral time scales of *C. elegans*.

1. Introduction

Caenorhabditis elegans is a free-living transparent worm, about 1 mm in length, that inhabits temperate environments across the Earth. The nematode is often found in rotting fruits and vegetables, since it feeds on the bacteria that reside in there (Schulenburg and Félix, 2017). C. elegans displays many of the basic features that are essential in human biology, which includes temperature and chemical sensing, learning, aging, and a number of disorders (Iliff and Xu, 2020; Goodman and Sengupta, 2018; Rankin et al., 1990; Tissenbaum, 2015; Kaletta and Hengartner, 2006; Markaki and Tavernarakis, 2010). This makes C. elegans a sufficiently complex animal model for studying problems pertaining to humans, and vet amenable enough for experimental accessibility and mathematical representation. The connectome of C. elegans has been resolved in its entirety (White et al., 1986; Varshney et al., 2011), resulting in the identification of 302 neurons, all the chemical synapses (about 5000), all neuromuscular junctions (about 2000), and all gap junctions (about 500). Out of the 302 neurons total, 20 are located in the pharynx, with the remaining 282 distributed among the head, the tail and along the ventral cord. Of these 282 neurons, 68 are sensory, equipped to detect chemicals, tactile stimuli and temperature (Edwards et al., 2008; Ghosh et al., 2021; Krieg et al., 2015; Russell et al., 2014; Rezai et al., 2010; Vidal-Gadea et al., 2015), with a large fraction of them located in the head ganglia. They extend their dendrites to the tip of the presumed nose (Allen et al., 2015), and display dense innervation with sensory structures.

While there has been extensive experimental work directed at shedding light on how C. elegans responds to environmental changes in temperature (Goodman and Sengupta, 2018; Mori and Ohshima, 1995; Clark et al., 2006; Ramot et al., 2008; Kimata et al., 2012), not as much has been done on the mathematical modeling front (Tsukada et al., 2016). Given the relevance of the matter, the aim of the work presented here is to obtain a better understanding of the mechanisms underlying the response of C. elegans to cold and heat. Our approach consists of embedding temperature features on a set of differential equations originally developed for mimicking the output of the C. elegans salt sensing, amphid single-ciliated right (ASER) neuron (Kuramochi and Doi, 2017), to obtain a mathematical representation of the C. elegans amphid finger-like (AFD) neurons. The AFD neurons are a pair of bilaterally symmetric, bipolar neurons that terminate in modified ciliated sensory endings, and have been demonstrated to be necessary for thermotaxis (Mori and Ohshima, 1995; Ramot et al., 2008; Ryu and Samuel, 2002; Kuhara et al., 2011). Genes needed for temperature sensing in C. elegans have been identified by classical genetic screens, and profiling of gene expression has revealed those expressed in AFD to be necessary for thermal sensing and orientation (Nishida et al., 2011). C. elegans is capable of detecting temperature variations as low as 0.1 °C or less, over a range of about 10 °C (Goodman and Sengupta, 2018; Ryu and Samuel, 2002). The animal displays a sophisticated migration behavior in locations with temperature gradient, using memory of the temperature in which it was developed, the cultivation temperature

^{*} Corresponding author at: Department of Physics, Illinois State University, Normal, 61790, IL, USA.

E-mail addresses: zmobille3@gatech.edu (Z. Mobille), rfollma@ilstu.edu (R. Follmann), avidal@ilstu.edu (A. Vidal-Gadea), erosa@ilstu.edu (E. Rosa Jr.).

Z. Mobille et al. BioSystems 223 (2023) 104814

 T_C , as Ref. Tsukada et al. (2016) and Kobayashi et al. (2016). In places with temperature above T_C the animal navigates toward lower temperature regions, in places with temperature below T_C the animal moves to regions at higher temperature or displays ataxia, and in regions with temperature close to T_C the animal follows isotherms around T_C (Kimata et al., 2012; Hedgecock and Russell, 1975). This higher tolerance to cold compared to heat (Takeishi et al., 2020; Ikeda et al., 2021) extends to the frozen C. elegans' capability of resuming normal life after being defrosted. Given the option C. elegans would stay cool, not warm.

The numerical simulation results presented here demonstrate how a relatively simple mathematical model can mimic the calcium dynamics of an in vivo AFD neuron during temperature experiments. We use color maps in Arrhenius-based parameter space to study how our model neuron responds to temperature variations, displaying ataxia or migration toward regions at its cultivation temperature when placed under conditions of temperature gradient (Kobayashi et al., 2016), in addition to the stereotypical 20-s duration of phasic AFD calcium activity measured experimentally by Tsukada et al. (2016). We also perform simulations for the behavior of worms cultivated at distinct temperatures and subject to temperatures incremented linearly, as well as oscillating temperatures combined with linear increases. Our studies suggest that, experimentally observed intracellular activity as a result of oscillatory increments in temperature, might be a direct outcome of oscillating inputs to the cyclic-nucleotide-gated ion channels in the dendrite, dependent upon the overall slope of the temperature gradient combined with a positive instantaneous rate of change in temperature (Kuhara et al., 2011). Although these conditions have been stated previously (Aoki and Mori, 2015), the work presented here is to our knowledge the first study that implements them in a concrete quantitative mathematical framework for temperature-generated calcium activity in the AFD neuron.

2. Model equations

The model equations we use in this study were originally developed for mimicking the behavior of the salt sensing ASER neuron in *C. elegans*, containing a simple step-down stimulus of NaCl concentration (Kuramochi and Doi, 2017). We extend this model by incorporating Arrhenius factors to account for the response of the thermosensitive AFD neuron to temperature. It is a compartmentalized model (Kuramochi and Doi, 2017) that depicts the AFD neuron as composed of dendrite, soma and axon, reciprocally coupled in a linear chain configuration. A schematic representation of the *C. elegans* is shown in Fig. 1(A) with the three AFD compartments indicated.

The model equations involve dimensionless variables representing calcium ion concentrations for the dendrite (c_d) , soma (c_s) and axon (c_a) ,

$$\frac{\mathrm{d}c_d}{\mathrm{d}t} = \frac{\rho}{\tau_d} \left[-c_d + y_d + D(W_d c_s - c_d) + I(t) \right],\tag{1}$$

$$\frac{dc_s}{dt} = \frac{1}{\tau_s} \left[-c_s + Y_s y_s + D(c_d + c_a - 2c_s) \right],$$
(2)

$$\frac{\mathrm{d}c_a}{\mathrm{d}t} = \frac{1}{\tau_a} \left[-c_a + Y_a y_a + D(W_a c_s - c_a) \right],\tag{3}$$

with reciprocal diffusive coupling between dendrite and soma, and between soma and axon, represented by the dimensionless parameter D=7.3. Parameters $\tau_d=15$ s, $\tau_s=3.7$ s and $\tau_a=1.2$ s are the time constants of calcium decay for the dendrite, soma, and axon, respectively. These are the only quantities in this mathematical model with explicit physical dimensions. All three compartments yield similar outputs (Fig. 1(B)) with a short delay between them.

The dimensionless quantity I(t) represents a direct input to the thermally-sensitive dendrites in the form of calcium influx, initially set constant for the extent of its duration. We set I=1 when the dendrite is exposed to an ambient temperature $T \neq T_C$. Otherwise, I=0. W_d and

 W_a are weights for calcium diffusion from the soma to the dendrite and from the soma to the axon, respectively. The values of these weights vary between 0 and 1, depending on the relative calcium activities of dendrite and axon. When both activities are zero, $c_d=c_a=0$, both weights are zero $W_d=W_a=0$. When at least one of the activities is non-zero $c_d\neq 0$ or $c_a\neq 0$ the weights are not identically zero. More details on W_d and W_a can be found in the Table 1. Parameters $Y_s=-0.224$ and $Y_a=-0.047$ control the magnitude of the inactivation variables y_s and y_a for the soma and axon respectively. The inactivation equation for the ith compartment is

$$\frac{dy_i}{dt} = -\phi A c_i, \quad i = d, s, a, \tag{4}$$

where A represents the time scale of the inactivation variables y_i . Large values of A produce faster inactivation, and vice-versa. Temperature effects on calcium activity responses are accounted for by the Arrhenius-based scaling parameters $\rho = \rho_0^{(T-T_C)/10}$ and $\phi = \phi_0^{(T-T_C)/10}$ (Connors, 1990), where ρ_0 and ϕ_0 are the Q_{10} temperature coefficients for activation and inactivation, respectively (Burek et al., 2019; Song et al., 2019). The temperature factors ρ and ϕ are incorporated solely in the dendrite, known to be the locus for C. elegans temperature sensing, as demonstrated by Chung et al. (2006). They used laser ablation for severing individual AFD's sensory neurons, a procedure that permanently damaged thermosensitivity behavior in the animal. In the implementation done here, we initially set $\rho_0 = 1.3$ and $\phi_0 = 3.0$ (Burek et al., 2019) for the dendrite, and $\phi_0 = 1.0$ for the soma and axon. T is the ambient temperature surrounding the cell, and the cultivation temperature is set initially to $T_C = 20$ °C.

The Q_{10} temperature coefficient was primarily introduced as a measure of how the speed of a chemical reaction is affected by a 10 °C change in temperature. It represents the ratio between the rate of a chemical reaction at a given temperature and the rate of that chemical reaction at a temperature $10\,^{\circ}$ C lower. Since its inception, Arrhenius' empirical relationship (Arrhenius, 1889) has been applied to a range of processes associated with temperature variations including muscle performance (Bennett, 1984), diffusion coefficients (O'Connell and McKenna, 1999), crystal vacancies population (Manning et al., 1997) and neuronal processes (Finke et al., 2011). For simplicity without lacking generality, and considering that the dendrite is the essential component of the AFD for temperature sensing (Chung et al., 2006), we center our attention on the output of the dendrite only.

The temperature sensitivity of the AFD neuron has been experimentally quantified by membrane electrophysiology (Ramot et al., 2008) and intracellular calcium dynamics (Clark et al., 2007). In our numerical simulations, the thermally-induced changes are directly related to the dendritic [Ca²⁺] output. This is illustrated in Fig. 2, showing the influence of temperature on the time $t_{\rm peak}$ it takes for the intracellular calcium activity in the dendrite to reach its maximum value from the start of a given stimulus. In this figure, the normalized responses of the dendrite intracellular concentration of calcium ions to a 60-s constant stimulus at three different temperatures, 30 °C, 20 °C and 10 °C, yield the respective peak times $t_{\rm peak}$ of 15.5 s, 18.4 s and 22.0 s, suggesting slower calcium response for $T < T_C$ and faster response for $T > T_C$. In short, the lower the temperature the slower the AFD response. This means that the speed of transfer of information from AFD to interneurons associated with locomotion is less for lower temperatures.

3. Temperature coefficients

In this section, we investigate the effects of temperature along with the coefficients ρ_0 and ϕ_0 on the calcium peak time response, as well as the half time peak of decay. Initially, we show results of simulations where the model neuron is presented with an instantaneous step-like stimulus from I(t)=0 to I(t)=1, and calculate the amount of time $t_{\rm peak}$ it takes for the dendritic calcium activity to reach its

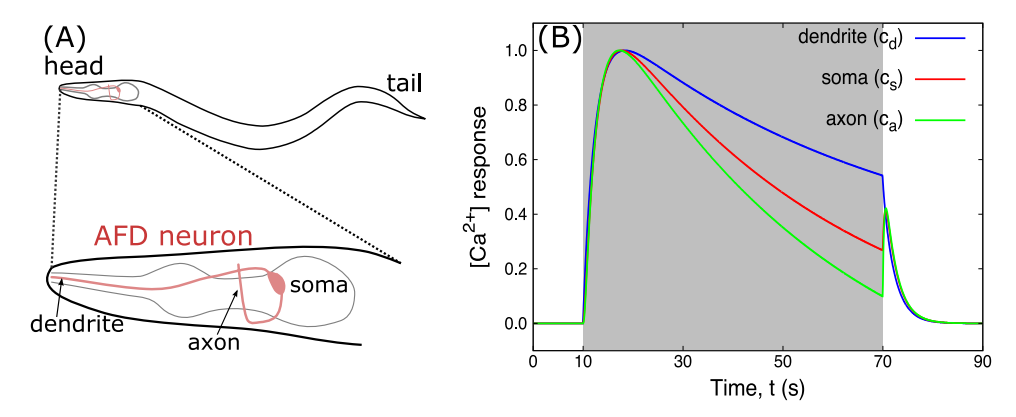


Fig. 1. (A) Schematic representation of *C. elegans* showing the AFD neuron in the head, indicating the dendrite, soma and axon. (B) Normalized calcium response of the dendritic, soma and axon compartments to a 60-s pulse of I(t) = 1 with temperature at its cultivation value $T_C = 20$ °C.

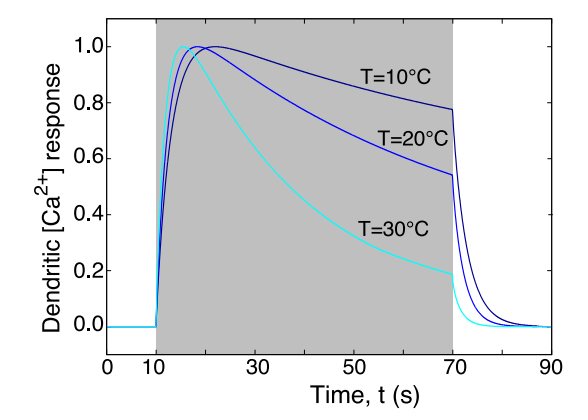


Fig. 2. Normalized calcium response of the dendritic compartment to a 60-s pulse of I(t)=1 at three different temperatures as indicated, with $\rho_0=1.3,\ \phi_0=3.0$ and $T_C=20$ °C.

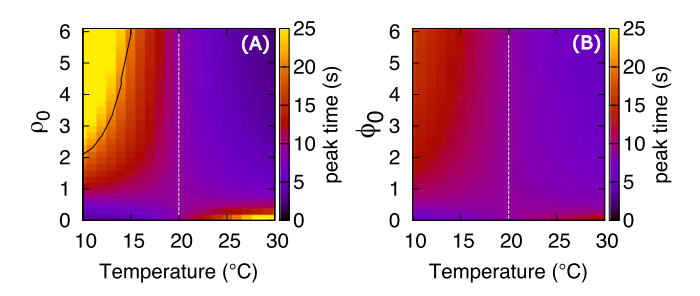


Fig. 3. Peak times of the dendritic calcium response when stimulated by an instantaneous step-like input from I(t)=0 to I(t)=1, for different ambient temperatures T and Arrhenius coefficients ρ_0 , ϕ_0 . (A) Effect of different combinations of ρ_0 and temperature T on the dendrite calcium activity peak time t_{peak} , with fixed $\phi_0=3.0$. The black solid line shows the *locus* of $t_{peak}=20$ s. (B) Different values of ϕ_0 with fixed $\rho_0=1.3$. The vertical dashed lines at $T_C=20$ °C indicate the boundary between parameter space areas for T below and above T_C .

maximum. These computational studies are motivated by biological experiments performed by Tsukada et al. (2016), who observed that transient AFD calcium responses to variations in temperature above some threshold typically last around 20 s, in worms that are freely navigating a temperature gradient. We interpret the stimulus I(t)=1 to represent a sufficiently fast and large change in temperature, with the Arrhenius functions $\rho(T)$ and $\phi(T)$ accounting explicitly for temperature effects.

The color maps of Fig. 3 show how the peak time t_{peak} of AFD calcium activity in our model varies in relation to T, ρ_0 , and ϕ_0 . The black line on the upper left-hand side of Fig. 3(A) denotes the contour

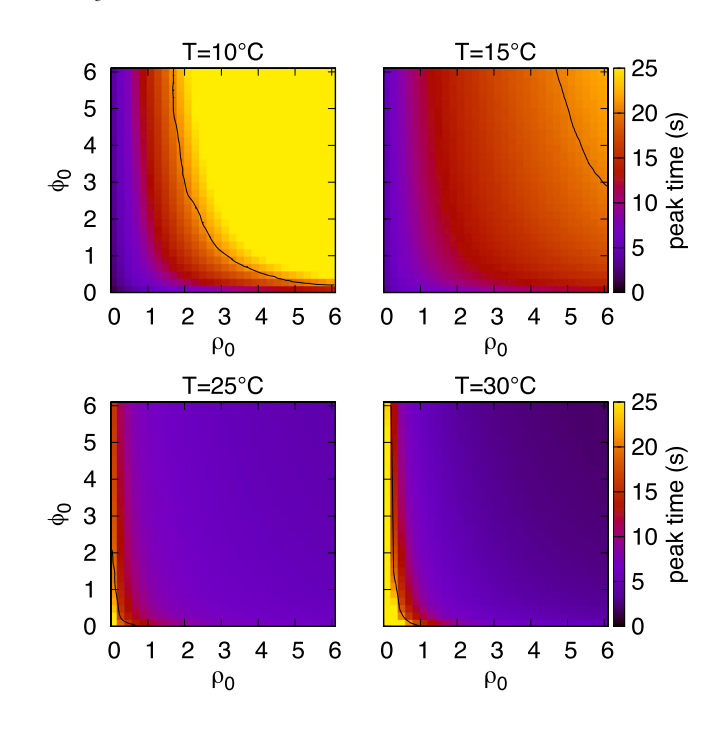


Fig. 4. Combined effects of ρ_0 and ϕ_0 on the dendritic peak time t_{peak} for four distinct temperature values, as indicated. The black line marks the values of ρ_0 and ϕ_0 for $t_{peak}=20$ s.

of constant $t_{\rm peak}$ = 20 s. The T and ρ_0 values contained within the yellowish area delimited by this line correspond to models where the neuron takes long enough time to reach peak calcium activity, so that the duration of the resulting calcium transient would be longer than the stereotypical 20-s pulses observed in Ref. Tsukada et al. (2016). Notably, this curve is only present at temperatures below about 15 °C for the values of ρ_0 tested, which is 5 °C or more, lower than the cultivation temperature $T_C = 20$ °C. If held constant, such a cold temperature would not allow AFD neurons to elicit a calcium transient, in accordance with known experimental results (Kobayashi et al., 2016). The output of the computational work displayed in Fig. 3(A) infers that AFD neurons initialized at sub-threshold temperatures will display slow calcium responses to quick pulses of large upward temperature deflections. In Fig. 3, color map (B) compared to (A) suggests that, for a range of T values, the peak time varies less with respect to changes in ϕ_0 than to changes in ρ_0 , emphasizing the notion that ϕ_0 modulates the calcium response inactivation more predominantly than the activation.

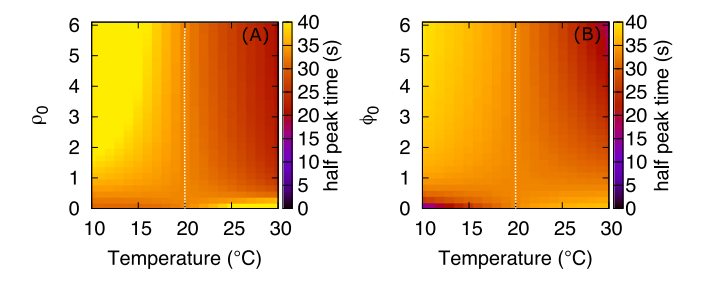


Fig. 5. Half decay times of the dendritic calcium response when stimulated by an instantaneous step-like input from I(t)=0 to I(t)=1, for different ambient temperatures T and Arrhenius coefficients ρ_0 (fixed $\phi_0=3.0$) in graph (A) and ϕ_0 (fixed $\rho_0=1.3$) in graph (B).

Whereas Fig. 3(A) and (B) demonstrate how ρ_0 and ϕ_0 independently modulate the peak time t_{peak} of calcium activity during a steplike input of I(t) = 1, Fig. 4 shows how ρ_0 and ϕ_0 combine to enable models that have various sensitivities to changes in ambient temperature. For a temperature of T = 10 °C there is a large area in parameter space that results in model AFD neurons which t_{neak} exceeds 20 s (large yellow area above the off diagonal on the top left graph of Fig. 4). As the ambient temperature increases toward T_C , at T = 15 °C this area for $t_{peak} = 20$ s decreases substantially, vanishing completely for $T = T_C = 20$ °C. These two examples of $T < T_C$ (10 °C and 15 °C) demonstrate the existence of combinations of ho_0 and ϕ_0 values that yield model neurons with a slow calcium response. Our simulations therefore suggest that in this case the animal would display ataxia, not seeking regions with higher temperatures, in agreement with behavior observed during in vivo experiments with freely-crawling worms in temperatures that are a few degrees lower than T_C (Tsukada et al.,

As the temperature increase continues above 20 °C, the $t_{peak} > 20$ s area resurfaces, now at the lower left corner of the graph for T=25 °C. This sliver-like parameter space area further increases, but not much for T=30 °C, indicating a narrow range of values for $\rho_0<1$ that correspond to models with $t_{\rm peak}>20$ s (two bottom graphs of Fig. 4). The parameter space in this sliver involving $\rho_0<1$ refers to biochemical processes that slow down at higher temperatures. Such an nonintuitive temperature dependence is rare, but not unprecedented (Revell and Williamson, 2013). Here, our focus is confined to the subsets of Fig. 4 where $\rho_0>1$ and $\phi_0>1$, in which case Fig. 4 shows that the model AFD neuron always responds within the 20-s time window when the ambient temperature is sufficiently high.

Figs. 3 and 4 display color maps indicating that the peak time varies less with respect to changes in ϕ_0 than for changes in ρ_0 , especially for temperatures above T_C , supporting the notion that ϕ_0 modulates more prominently the inactivation of the calcium response, compared to the activation. In order to verify this aspect of AFD's calcium response, we generate color maps featuring how the half decay time $t_{1/2}^{decay}$ changes with variations in T, ρ_0 and ϕ_0 . The half decay time is measured as the time it takes for the maximum calcium response amplitude decay to one half of its value, in connection with its value at the ending time of the stimulus I(t). Fig. 5 shows the half decay peak time (color bar) changes for a range of ρ_0 and temperature (graph A) and for a range of ϕ_0 and temperature (graph B). While in Fig. 3B the changes in peak time elicited in connection with ϕ_0 are substantially less than those changes elicited in connection with ρ_0 , the corresponding graphs in Fig. 5 show that the changes elicited in the $t_{1/2}^{decay}$ in connection with ϕ_0 are not much dissimilar from each other.

The color maps presented in this section may be useful to guide further modeling studies that are tightly coupled to experiments designed for obtaining actual parameter values for ρ_0 and ϕ_0 . This kind of study would complement works of the type of Ramot et al. (2008), who obtained a value of $Q_{10}\approx 10$ for the activation rate ρ_0 , and of ≈ 2.8 for the

inactivation rate ϕ_0 in the ionic currents in AFD. These thermo-sensitive ionic currents are likely coupled to the thermo-sensitive calcium dynamics modeled here. The nature of this coupling presents an important unsolved problem in the *C. elegans* thermoreception literature, and would likely benefit from a combined experimental/theoretical study of the underlying biophysics that is articulated in this work.

4. Temperature gradient effects

Experimental studies concerning the dynamics of a cyclic-nucleotide-gated (CNG) ion channel expressed by the AFD neuron of C. elegans (Clark et al., 2006; Li et al., 2017) suggest a temperature-dependent stimulus I(T) to the dendrite that is only significant above some threshold temperature value; this quantity I(T) replaces the quantity I(t) in Eq. (1) for the results in this section. Additionally, the CNG channel, encoded by the tax-2 and tax-4 genes, has been shown to be critical for thermotaxis in C. elegans (Inada et al., 2006). To account for this, we introduce a sigmoidal function as a model for how temperature is transduced into dendritic input by the CNG ion channel. The temperature-dependent input stimulus is therefore modeled as

$$I(T) = \frac{1}{1 + a^{\alpha(T^* - T)}} \tag{5}$$

where the parameter $\alpha=8$ determines the slope of the curve and $T^*=T_C-1$ °C corresponds to the curve's midpoint temperature. This model is consistent with the empirical fact that AFD calcium influx occurs only when the ambient temperature is above a threshold temperature that is 2 °C less than the cultivation temperature; symbolically, $T=T_C-2$ °C (Aoki and Mori, 2015). Deregulation of the threshold temperature associated with thermo-receptor currents is observed upon genetic deletion of the phosphodiesterase-2 (PDE-2) in AFD (Wang et al., 2013). Thus, this relation between T^* and T_C rests upon proper functioning of PDE-2. In addition to being above the threshold T_C-2 °C, the temperature must be increasing in a given moment for the calcium influx to AFD to be non-zero (Aoki and Mori, 2015). This is discussed more, below.

We initially run simulations for a continuous linear increase in temperature from 14 °C to 24 °C over a time interval of 200 s. The corresponding dendritic outputs for three different cultivation temperatures are shown in Fig. 6. The post-ramp elevated Ca²⁺ steady state is obtained by setting $dy_i/dt = 0$ when dT/dt = 0, for i = 0d, s, a. The inactivation of AFD's calcium may still change when the temperature is constant, but on a much smaller time-scale compared to the time-scale of the change in temperature used in this experiment. We find a one-to-one match with experimental results for in vivo AFD neurons' response temperatures with peak responses happening for the corresponding 17 °C, 20 °C and 23 °C cultivation temperatures (see Fig. 1E in Ref. Kobayashi et al. (2016)). As the temperature increases, the peak time for each curve happens at the respective cultivation temperatures (Kobayashi et al., 2016). This suggests that in addition to the known network synaptic plasticity mechanism for memory in the brain (Hebb, 2005), neuronal memory response can also be manifested in less complex systems as is the case here for cultivation temperature in a single neuron (Kobayashi et al., 2016). While our model does not account for the biophysical mechanisms underlying single-cell memory of T_C in AFD, it does produce the correct calcium response to a temperature ramp, given that this memory already exists. Furthermore, the post-stimulus elevated Ca2+ steady states present in our Fig. 6 simulations suggest a possible mechanism for short-term memory of super-threshold stimuli. Namely, that C. elegans encodes temperatures above its threshold with an elevated baseline calcium level. Interestingly, the membrane voltage of the AFD neuron follows this same trend with respect to temperature (see Figure 1b of Ref. Ramot et al. (2008)).

Besides the peak times of the three calcium responses shown in Fig. 5, the decay rates are also worth noting. Due to the combination of the inactivation Arhennius function $\phi(T)$ and the threshold T^* in Eq. (5), the decay rates are slightly faster for traces with higher cultivation

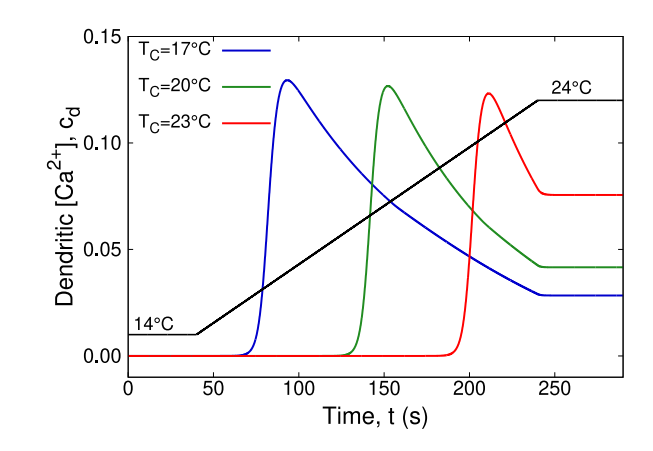


Fig. 6. Linear increase in temperature from 14 °C to 24 °C (black line), and the corresponding calcium responses for cultivation temperatures of 17 °C, 20 °C, and 23 °C, color coded as indicated. This computational result forms a direct match with the experimental output depicted in Fig. 1E of Ref. Kobayashi et al. (2016).

temperatures. While this prediction appears somewhat valid for predicting the experimental calcium responses of dissected AFD neurons to a temperature ramp (Figure 1f of Ref. Kobayashi et al. (2016)), it seems to apply less to the *in vivo* case (Figure 1e of Ref. Kobayashi et al. (2016)).

Next, we add small amplitude oscillations on top of the linearly increasing temperature to test how the AFD bidirectional thermosensory response allows the neuron to transduce sensory input into motor output. This results in phase synchronization (Rosa et al., 1998; Neiman and Russell, 2002; Zhou et al., 2021) of its calcium dynamics with the oscillatory temperatures (Clark et al., 2006). The feature is implemented in our model by imposing a small oscillatory component on a linear increase in temperature given by

$$T(t) = 0.01t + 0.1\sin(2\pi t/15) + 15$$
(6)

starting at 15.5 °C going up to 19.5 °C (Fig. 7). This type of temperature stimulus would be naturally perceived by a worm crawling with its typical undulatory movement on a sufficiently steep temperature gradient (Gray and Lissmann, 1964; Niebur and Erdös, 1991). The oscillatory stimulus elicits a corresponding oscillatory calcium response, closely matching experimental observations from in vivo fluorescence studies (Clark et al., 2006), highlighting the ability of the AFD neuron to respond to temperature fluctuations with amplitudes as small as 0.1 °C or less. We obtained this result by including temperature sensitive CNG ion channel dynamics through use of Eq. (5), in conjunction with an alteration to the inactivation law. This alteration consists of the following: (1) we set $y_i = 0$ whenever $dT/dt \le 0$ and (2) we set I(T) = 0 whenever dT/dt = 0, otherwise I(T) is given by Eq. (5). Without this extra constraint, the temperature phase-locked dynamics are not observed. This computational result then suggests that a possible mechanism underlying the phase-locked oscillations (as observed experimentally in freely-moving worms by Clark et al. (2006, 2007)) would be that the temperature-evoked oscillations in local cyclic guanosine monophosphate (cGMP) concentration finely tune the permeability of CNG ion channels, thus altering the Ca²⁺ currents that flow through such channels. In turn, this changes the intracellular Ca2+ concentration of the neuron. Indeed, electrophysiological results (figure 1 of Ref. Ramot et al. (2008)) show that a large and fast depolarizing membrane current in AFD coincides with the ambient temperature increasing past its stored threshold. If this current is carried by calcium ions, then it is clear that temperatureevoked changes in [Ca²⁺] are mediated, or at least initiated, by calcium influx from the extracellular space. Temperature-evoked changes in cGMP could also evoke free Ca²⁺ from internal stores such as the endoplasmic reticulum, mitochondria, or buffers (Keener and Sneyd, 2009).

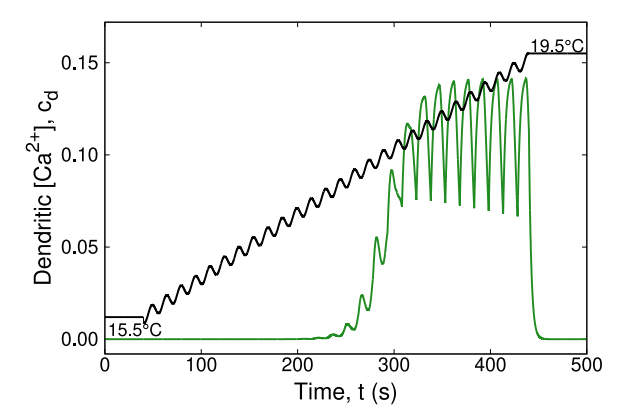


Fig. 7. Calcium response (green line) for an oscillating temperature increase as indicated by the black line between 15.5 °C and 19.5 °C. This computational result is directly related to the experimental output depicted in Fig. 2B (bottom) of Ref. Clark et al. (2006).

It is possible that low-amplitude [Ca²⁺] oscillations are modulated by internal stores while the large wave that those oscillations ride (as in Fig. 7) comes from the large transmembrane current observed by Ramot et al. (2008). The modeling work undertaken here demonstrates that both of these aspects can be described accurately with a set of relatively simple differential equations and the nonlinear temperature transduction function I(T). The modifications of the inactivation law needed to obtain our oscillatory plot, as described above, imply that the AFD thermotransduction machinery has a method for computing the sign of $\mathrm{d}T/\mathrm{d}t$, as well as the difference of the ambient temperature from the cultivation temperature.

5. Concluding remarks

Temperature plays a major role in the regulation of behavior in biological organisms in general, with Caenorhabditis elegans not being an exception. The nematode's relatively small and simple neuronal system, but displaying features typically encountered in more complex organisms including humans, has made it widely used as a tractable animal model for studying behavior in living systems. Our focus here is on how temperature-regulated behavior results from worm's neural activity. We implement temperature Arrhenius factors on a mathematical model originally developed for studying a salt sensing neuron (ASER), aiming at developing equations that represent AFD neurons as the sensory processing center of thermal information for C. elegans. Even though the extensive studies already done, how the AFD neurons generate calcium activity that temporally tracks temperature gradients is still unknown. For example, the study by Tsukada et al. (2016) focuses on fitting a linear-nonlinear (LN) convolution model to temperature-calcium time series data. While this approach characterizes the response function of AFD to temperature and has contributed significantly to more elaborate network modeling of the full thermotaxis circuit (Ikeda et al., 2021), it is not based on biophysical mechanism hypothesized to be the basis for AFD thermoreception. Additionally, the LN approach does not address the results of experiments with non-oscillatory temperature stimuli (Kobayashi et al., 2016).

The phenomenological modeling we present here accounts for AFD's thermally-induced calcium activity by asserting a dynamical mechanism without delving into the physiological details. It attempts to bridge the gap between descriptive models (Tsukada et al., 2016) and biophysically detailed ones for the AFD neuron (Naudin et al., 2021). Such biophysical modeling studies capture the membrane voltage and current of *C. elegans* neurons using a Hodgkin–Huxley formalism (Hodgkin and Huxley, 1952; Rutherford et al., 2020), without coupling these quantities to the temperature-dependent intracellular

Z. Mobille et al. BioSystems 223 (2023) 104814

calcium investigated in this work. It is known experimentally that both the membrane electrophysiology (Ramot et al., 2008) and intracellular calcium dynamics (Clark et al., 2006, 2007) in AFD are tightly correlated with changes in ambient temperature. A complete understanding of the mechanisms underlying temperature encoding by the AFD neuron will therefore require a theory that accounts for the interactions between these physiological quantities. The mathematical model of calcium dynamics developed here suggests that the thermoreceptor currents measured on the AFD dendrites by Ramot et al. (2008) interact with the calcium system in such a way as to raise the dendritic calcium time derivative by an amount given by Eq. (5), which is dependent on the temperature T. This fact implies that the thermoreceptor currents are either carried by calcium ions or initiate a process that results in calcium ion increase.

The model equations used in this work exhibit a biphasic $[Ca^{2+}]$ transient behavior (Fig. 1(B)) for soma and axon with the increase in $[Ca^{2+}]$ in the beginning of the stimulus and after the removal of the stimulus. This is an interesting feature encountered, for example, in ASH chemically sensory neurons (Chokshi et al., 2010; Mirzakhalili et al., 2018; Ferkey et al., 2021), and that in here emerges naturally. Preliminary investigations indicate a dependency of the biphasic behavior on the coupling parameter D and the diffusion weights W_a and W_d between the compartments. Preliminary testing of how robust the system is to variations in these parameters suggest that they are strong candidates for tuning the model equations to be applied to a range of physical conditions including temperature. This opens a wide window of possibilities for further exploring the potential of this compartmental model in the future.

In the original mathematical model developed for the chemosensitive ASER neuron (Kuramochi and Doi, 2017) that we build upon here, the parameters were fit using data from experiments performed on that neuron. Given that these parameters were changed minimally in our implementation of the AFD model, we speculate that the mechanism by which ASER [Ca2+] activates in response to fluctuations in NaCl has similarities to that of the mechanism by which AFD activates to temperature changes. Indeed, genetic studies support this claim since both ASER and AFD are known to rely on a common family of transmembrane proteins, the receptor guanylate cyclases (rGC's), to mediate their responses to NaCl and temperature, respectively (Ortiz et al., 2009; Inada et al., 2006). The rGC implicated in thermo-sensation in AFD is genetically distinct from the rGC implicated in chemo-sensation in ASER. However, they are both known to activate a second messenger signaling cascade mediated by cyclic guanosine monophosphate (cGMP). A sufficient change in intracellular cGMP activity subsequently triggers a change in permeability of the cGMP-gated nonselective cation channel encoded by the tax-2 and tax-4 genes (Komatsu et al., 1996). Our model results suggest that the sensory transduction mechanism, by which temperature oscillations cause phase-locked oscillations in AFD [Ca²⁺], may be analogous to the mechanism by which periodic fluctuations in extracellular NaCl cause phase-locked oscillations in ASER [Ca²⁺]. Whereas salt is the substrate by which rGC-amplified ion channel currents are initiated in the ASER neuron, heat is the corresponding agent in the AFD neuron. Since heat is not a physical object that binds to a post-synaptic receptor, there must be some condition in the post-synaptic space of AFD that a sufficient amount of heat renders ideal for the opening of thermoreceptor channels on the dendritic membrane.

In summary, our computational work asserts that (1) temperature-mediated calcium responses in the AFD neuron can be conceptualized as a biochemical process by which activation and inactivation are separately modulated by the Arhennius functions $\rho=\rho(T)$ and $\phi=\phi(T)$, respectively, and (2) one way for mimicking *in vivo* results of the AFD neuron during temperature gradient experiments using this phenomenological model is to increase the time derivative of the dendritic calcium by an amount I=I(T) given by Eq. (5), assuming that the temperature is increasing $(\mathrm{d}T/\mathrm{d}t>0)$ in that moment; otherwise, set

Table 1 Calcium diffusion weights W_d and W_a . Source: Adapted from table 1 of Ref. Kuramochi and Doi (2017).

	$c_a > 0$	$c_{a} < 0$	$c_a = 0$
$c_d > 0$	$W_d = \frac{ c_a }{ c_d + c_a }$	$W_d = 0$	$W_d = \frac{ c_a }{ c_d + c_a }$
	$W_a = \frac{ c_d }{ c_d + c_a }$	$W_a = 1$	$W_a = \frac{ c_d }{ c_d + c_a }$
$c_d < 0$	$W_d = 1$	$W_d = \frac{ c_d }{ c_d + c_a }$	$W_d = 1$
	$W_a = 0$	$W_a = rac{ c_a }{ c_d + c_a }$	$W_a = 0$
$c_d = 0$	$W_d = 0$	$W_d = 0$	$W_d = 0$
	$W_a = 1$	$W_a = 1$	$W_a = 0$

I(T)=0 as well as the inactivation $y_i=0$ for i=d,s,a. Future modeling studies implementing these rules may be able to explain them via physical mechanisms. Experiments monitoring *in vivo* calcium activity in the AFD neuron during temperature pulses may use this model to find the best fit of ρ_0 and ϕ_0 to their data. Finally, we emphasize the relevance of studies involving temperature related behaviors, as is the case of this present work, in the context of climate change. Acclimatization and migration (Ohnishi et al., 2020) capabilities have already become ever more crucial to the survival of many species.

Declaration of competing interest

The authors declare that they have no known competing financial interests or personal relationships that could have appeared to influence the work reported in this paper.

Acknowledgments

Research reported in this publication was supported in part by the National Institute of General Medical Sciences of the National Institutes of Health under award number T32GM142616 and the by NSF Grant 1818140 to A.G.V.-G.

References

Allen, E., Ren, J., Zhang, Y., Alcedo, J., 2015. Sensory systems: their impact on *C. elegans* survival. Neuroscience 296, 15–25.

Aoki, I., Mori, I., 2015. Molecular biology of thermosensory transduction in C. elegans. Curr. Opin. Neurobiol. 34, 117–124.

Arrhenius, S., 1889. Über die dissociationswärme und den einfluss der temperatur auf den dissociationsgrad der elektrolyte. Z. Phys. Chem. 4 (1), 96–116, A translation of part of this paper is included in Back, M.H., and Laidler, K.J., Selected Readings in Chemical Kinetics, Pergamon Press, Oxford, 1967, pp. 31–35..

Bennett, A., 1984. Thermal dependence of muscle function. Am. J. Physiol. Regul. Integr. Comp. Physiol. 247 (2), R217–R229.

Burek, M., Follmann, R., Rosa, E., 2019. Temperature effects on neuronal firing rates and tonic-to-bursting transitions. Biosystems 180, 1–6.

Chokshi, T.V., Bazopoulou, D., Chronis, N., 2010. An automated microfluidic platform for calcium imaging of chemosensory neurons in Caenorhabditis elegans. Lab Chip 10 (20), 2758–2763.

Chung, S.H., Clark, D.A., Gabel, C.V., Mazur, E., Samuel, A.D., 2006. The role of the AFD neuron in *C. elegans* thermotaxis analyzed using femtosecond laser ablation. BMC Neurosci. 7 (1), 1–11.

Clark, D.A., Biron, D., Sengupta, P., Samuel, A.D., 2006. The AFD sensory neurons encode multiple functions underlying thermotactic behavior in *Caenorhabditis* elegans. J. Neurosci. 26 (28), 7444–7451.

Clark, D.A., Gabel, C.V., Gabel, H., Samuel, A.D., 2007. Temporal activity patterns in thermosensory neurons of freely moving *Caenorhabditis elegans* encode spatial thermal gradients. J. Neurosci. 27 (23), 6083–6090.

Connors, K.A., 1990. Chemical Kinetics: The Study of Reaction Rates in Solution. Wiley-VCH Verlag GmbH.

Edwards, S.L., Charlie, N.K., Milfort, M.C., Brown, B.S., Gravlin, C.N., Knecht, J.E., Miller, K.G., 2008. A novel molecular solution for ultraviolet light detection in *Caenorhabditis elegans*. PLoS Biol. 6 (8), e198.

Ferkey, D.M., Sengupta, P., L'Etoile, N.D., 2021. Chemosensory signal transduction in Caenorhabditis elegans. Genetics 217 (3), 1–35. Z. Mobille et al. BioSystems 223 (2023) 104814

- Finke, C., Freund, J.A., Rosa Jr., E., Bryant, P.H., Braun, H.A., Feudel, U., 2011.
 Temperature-dependent stochastic dynamics of the Huber-Braun neuron model.
 Chaos 21 (4) 047510
- Ghosh, D.D., Lee, D., Jin, X., Horvitz, H.R., Nitabach, M.N., 2021. *C. elegans* discriminates colors to guide foraging. Science 371 (6533), 1059–1063.
- Goodman, M.B., Sengupta, P., 2018. The extraordinary AFD thermosensor of C. elegans. Pflügers Archiv. Eur. J. Physiol. 470 (5), 839–849.
- Gray, J., Lissmann, H.W., 1964. The locomotion of nematodes. J. Exp. Biol. 41 (1), 135–154.
- Hebb, D.O., 2005. The Organization of Behavior: A Neuropsychological Theory. Psychology Press.
- Hedgecock, E.M., Russell, R.L., 1975. Normal and mutant thermotaxis in the nematode *Caenorhabditis elegans*. Proc. Natl. Acad. Sci. 72 (10), 4061–4065.
- Hodgkin, A.L., Huxley, A.F., 1952. A quantitative description of membrane current and its application to conduction and excitation in nerve. J. Physiol. 117 (4), 500.
- Ikeda, M., Matsumoto, H., Izquierdo, E.J., 2021. Persistent thermal input controls steering behavior in Caenorhabditis elegans. PLoS Comput. Biol. 17 (1), e1007916.
- Iliff, A.J., Xu, X.S., 2020. *C. elegans*: a sensible model for sensory biology. J. Neurogenet. 34 (3–4), 347–350.
- Inada, H., Ito, H., Satterlee, J., Sengupta, P., Matsumoto, K., Mori, I., 2006. Identification of guanylyl cyclases that function in thermosensory neurons of *Caenorhabditis elegans*. Genetics 172 (4), 2239–2252.
- Kaletta, T., Hengartner, M.O., 2006. Finding function in novel targets: C. elegans as a model organism. Nat. Rev. Drug Discov. 5 (5), 387–399.
- Keener, J., Sneyd, J., 2009. Mathematical Physiology 1: Cellular Physiology, Vol. 2. Springer, New York, NY, USA.
- Kimata, T., Sasakura, H., Ohnishi, N., Nishio, N., Mori, I., 2012. Thermotaxis of C. elegans as a model for temperature perception, neural information processing and neural plasticity. In: Worm, Vol. 1. Taylor & Francis, pp. 31–41.
- Kobayashi, K., Nakano, S., Amano, M., Tsuboi, D., Nishioka, T., Ikeda, S., Yokoyama, G., Kaibuchi, K., Mori, I., 2016. Single-cell memory regulates a neural circuit for sensory behavior. Cell Rep. 14 (1), 11–21.
- Komatsu, H., Mori, I., Rhee, J.-S., Akaike, N., Ohshima, Y., 1996. Mutations in a cyclic nucleotide-gated channel lead to abnormal thermosensation and chemosensation in *C. elegans*. Neuron 17 (4), 707–718.
- Krieg, M., Dunn, A.R., Goodman, M.B., 2015. Mechanical systems biology of C. elegans touch sensation. BioEssays 37 (3), 335–344.
- Kuhara, A., Ohnishi, N., Shimowada, T., Mori, I., 2011. Neural coding in a single sensory neuron controlling opposite seeking behaviours in *Caenorhabditis elegans*. Nature Commun. 2 (1), 1–9.
- Kuramochi, M., Doi, M., 2017. A computational model based on multi-regional calcium imaging represents the spatio-temporal dynamics in a *Caenorhabditis elegans* sensory neuron. PLoS One 12 (1), e0168415.
- Li, M., Zhou, X., Wang, S., Michailidis, I., Gong, Y., Su, D., Li, H., Li, X., Yang, J., 2017. Structure of a eukaryotic cyclic-nucleotide-gated channel. Nature 542 (7639), 60–65
- Manning, P., Sirman, J., De Souza, R., Kilner, J., 1997. The kinetics of oxygen transport in 9.5 mol% single crystal yttria stabilised zirconia. Solid State Ion. 100 (1–2), 1–10.
- Markaki, M., Tavernarakis, N., 2010. Modeling human diseases in *Caenorhabditis elegans*. Biotechnol. J. 5 (12), 1261–1276.
- Mirzakhalili, E., Epureanu, B.I., Gourgou, E., 2018. A mathematical and computational model of the calcium dynamics in Caenorhabditis elegans ASH sensory neuron. PLoS One 13 (7), e0201302.
- Mori, I., Ohshima, Y., 1995. Neural regulation of thermotaxis in *Caenorhabditis elegans*. Nature 376 (6538), 344–348.
- Naudin, L., Corson, N., Aziz-Alaoui, M., Jiménez Laredo, J.L., Démare, T., 2021. On the modeling of the three types of non-spiking neurons of the *Caenorhabditis elegans*. Int. J. Neural Syst. 31 (02), 2050063.
- Neiman, A.B., Russell, D.F., 2002. Synchronization of noise-induced bursts in noncoupled sensory neurons. Phys. Rev. Lett. 88, 138103.

Niebur, E., Erdös, P., 1991. Theory of the locomotion of nematodes: dynamics of undulatory progression on a surface. Biophys. J. 60 (5), 1132–1146.

- Nishida, Y., Sugi, T., Nonomura, M., Mori, I., 2011. Identification of the AFD neuron as the site of action of the CREB protein in *Caenorhabditis elegans* thermotaxis. EMBO Rep. 12 (8), 855–862.
- O'Connell, P.A., McKenna, G.B., 1999. Arrhenius-type temperature dependence of the segmental relaxation below T_e . J. Chem. Phys. 110 (22), 11054–11060.
- Ohnishi, K., Saito, S., Miura, T., Ohta, A., Tominaga, M., Sokabe, T., Kuhara, A., 2020.
 OSM-9 and OCR-2 TRPV channels are accessorial warm receptors in *Caenorhabditis elegans* temperature acclimatisation. Sci. Rep. 10 (1), 1–14.
- Ortiz, C.O., Faumont, S., Takayama, J., Ahmed, H.K., Goldsmith, A.D., Pocock, R., McCormick, K.E., Kunimoto, H., Iino, Y., Lockery, S., et al., 2009. Lateralized gustatory behavior of *C. elegans* is controlled by specific receptor-type guanylyl cyclases. Curr. Biol. 19 (12), 996–1004.
- Ramot, D., MacInnis, B.L., Goodman, M.B., 2008. Bidirectional temperature-sensing by a single thermosensory neuron in *C. elegans*. Nature Neurosci. 11 (8), 908.
- Rankin, C.H., Beck, C.D., Chiba, C.M., 1990. *Caenorhabditis elegans*: a new model system for the study of learning and memory. Behav. Brain Res. 37 (1), 89–92.
- Revell, L.E., Williamson, B.E., 2013. Why are some reactions slower at higher temperatures? J. Chem. Educ. 90 (8), 1024–1027.
- Rezai, P., Siddiqui, A., Selvaganapathy, P.R., Gupta, B.P., 2010. Electrotaxis of Caenorhabditis elegans in a microfluidic environment. Lab Chip 10 (2), 220–226.
- Rosa, Jr., E., Ott, E., Hess, M.H., 1998. Transition to phase synchronization of chaos. Phys. Rev. Lett. 80 (8), 1642.
- Russell, J., Vidal-Gadea, A.G., Makay, A., Lanam, C., Pierce-Shimomura, J.T., 2014. Humidity sensation requires both mechanosensory and thermosensory pathways in Caenorhabditis elegans. Proc. Natl. Acad. Sci. 111 (22), 8269–8274.
- Rutherford, G.H., Mobille, Z.D., Brandt-Trainer, J., Follmann, R., Rosa Jr., E., 2020.

 Analog implementation of a Hodgkin–Huxley model neuron. Amer. J. Phys. 88 (11), 918–923.
- Ryu, W.S., Samuel, A.D., 2002. Thermotaxis in Caenorhabditis elegans analyzed by measuring responses to defined thermal stimuli. J. Neurosci. 22 (13), 5727–5733.
- Schulenburg, H., Félix, M.-A., 2017. The natural biotic environment of *Caenorhabditis elegans*. Genetics 206 (1), 55–86.
- Song, X., Wang, H., Chen, Y., Lai, Y.-C., 2019. Emergence of an optimal temperature in action-potential propagation through myelinated axons. Phys. Rev. E 100 (3), 032416.
- Takeishi, A., Takagaki, N., Kuhara, A., 2020. Temperature signaling underlying thermotaxis and cold tolerance in *Caenorhabditis elegans*. J. Neurogenet. 34 (3–4), 351–362.
- Tissenbaum, H.A., 2015. Using *C. elegans* for aging research. Invertebr. Repr. Dev. 59 (sup1), 59–63.
- Tsukada, Y., Yamao, M., Naoki, H., Shimowada, T., Ohnishi, N., Kuhara, A., Ishii, S., Mori, I., 2016. Reconstruction of spatial thermal gradient encoded in thermosensory neuron AFD in *Caenorhabditis elegans*. J. Neurosci. 36 (9), 2571–2581.
- Varshney, L.R., Chen, B.L., Paniagua, E., Hall, D.H., Chklovskii, D.B., 2011. Structural properties of the *Caenorhabditis elegans* neuronal network. PLoS Comput. Biol. 7 (2), e1001066.
- Vidal-Gadea, A., Ward, K., Beron, C., Ghorashian, N., Gokce, S., Russell, J., Truong, N., Parikh, A., Gadea, O., Ben-Yakar, A., et al., 2015. Magnetosensitive neurons mediate geomagnetic orientation in *Caenorhabditis elegans*. eLife 4, e07493.
- Wang, D., OâHalloran, D., Goodman, M.B., 2013. GCY-8, PDE-2, and NCS-1 are critical elements of the cGMP-dependent thermotransduction cascade in the AFD neurons responsible for *C. elegans* thermotaxis. J. Gener. Physiol. 142 (4), 437–449.
- White, J.G., Southgate, E., Thomson, J.N., Brenner, S., 1986. The structure of the nervous system of the nematode *Caenorhabditis elegans*. Philos. Trans. R. Soc. Lond. Ser. B Biol. Sci. 314 (1165), 1–340.
- Zhou, W., Hao, Z., Gravish, N., 2021. Collective synchronization of undulatory movement through contact. Phys. Rev. X 11 (3), 031051.